

## Synthesis of Chalcopyrite-type and Thiospinel Minerals/Materials by Low Temperature Melts of Xanthates

Malik Dilshad Khan,<sup>a,b</sup> Ghulam Murtaza,<sup>b</sup> Neerish Revaprasadu,<sup>a\*</sup> Paul O'Brien<sup>b,c\*</sup>

<sup>a</sup> Department of Chemistry, University of Zululand, Private Bag X1001, Kwa-dlangezwa, 3880, South Africa.

<sup>b</sup> School of Chemistry, The University of Manchester, Oxford Road, Manchester, M13 9PL.

<sup>c</sup> School of Materials, The University of Manchester, Oxford Road, Manchester, M13 9PL.

\*E-mail: [paul.o'brien@manchester.ac.uk](mailto:paul.o'brien@manchester.ac.uk)

### SUPPORTING INFORMATION

## **Experimental**

### **Materials**

The reagents and solvent *i.e.* Potassium ethyl xanthogenate,  $\text{AgNO}_3$ ,  $\text{BiCl}_3$ ,  $\text{CoCl}_2$ ,  $\text{CrCl}_3$ ,  $\text{Cu}(\text{NO}_3)_2 \cdot 3\text{H}_2\text{O}$ ,  $\text{Fe}(\text{NO}_3)_3 \cdot 9\text{H}_2\text{O}$ ,  $\text{GaCl}_3$ ,  $\text{InCl}_3$ ,  $\text{NiCl}_2 \cdot 6\text{H}_2\text{O}$ ,  $\text{SbCl}_3$ ,  $\text{SnCl}_2$  and methanol were procured from Sigma Aldrich and were used as received.

### **Synthesis of metal xanthate complexes**

The xanthate complexes of all the metals used in this study are well known and are reported in literature. The complexes were synthesized by standard metathetical methods, and the detailed synthesis is reported elsewhere.<sup>1-13</sup> The synthesized complexes were characterized by the elemental analysis, and the results were comparable with the reported literature.

**Ag(S<sub>2</sub>COEt)<sub>2</sub>.** Anal. Calcd for  $\text{C}_3\text{H}_5\text{OS}_2\text{Ag}$ : C, 15.71; H, 2.20; S, 27.93; Ag, 47.1%. Found: C, 15.82; H, 2.5; S, 28.2; Ag, 47.3%.

**Bi(S<sub>2</sub>COEt)<sub>3</sub>.** Elemental analysis (%) found for  $\text{C}_9\text{H}_{15}\text{S}_6\text{O}_3\text{Bi}$ : C, 19.1; H, 2.65; S, 33.46; Bi, 36.47. Calcd: C, 18.9; H, 2.64; S, 33.53; Bi, 36.49.

**Co(S<sub>2</sub>COEt)<sub>3</sub>.** Elemental analysis for  $\text{C}_9\text{H}_{15}\text{S}_6\text{O}_3\text{Co}$ , found (calc.) C: 25.5 (25.6); H: 3.6 (3.58); S: 45.44 (45.31).

**Cr(S<sub>2</sub>COEt)<sub>3</sub>.** Elemental analysis for  $\text{C}_9\text{H}_{15}\text{S}_6\text{O}_3\text{Cr}$ , found (calc.) C: 25.31 (25.98); H: 3.51 (3.63); S: 45.89 (46.2).

**Cu(S<sub>2</sub>COEt)<sub>2</sub>.** Elemental analysis for  $\text{C}_6\text{H}_{10}\text{O}_2\text{S}_4\text{Cu}$ : Found: C, 22.9; H, 3.2; S, 40.9; Cu, 20.5; Calc. C, 23.5; H, 3.3; S, 41.8; Cu, 20.8.

**Ga(S<sub>2</sub>COEt)<sub>3</sub>.** Elemental analysis found for  $\text{C}_9\text{H}_{15}\text{S}_6\text{O}_3\text{Ga}$ : C, 25.1; H, 3.40; S, 44.7; Calc. C, 24.92; H, 3.48; S, 44.31;

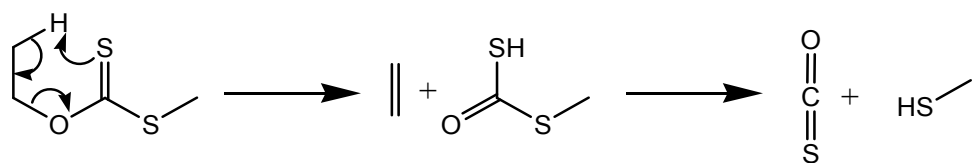
**Fe(S<sub>2</sub>COEt)<sub>3</sub>.** Elemental analysis found for  $\text{C}_9\text{H}_{15}\text{S}_6\text{O}_3\text{Fe}$ : C, 25.6; H, 3.4; S, 45.5; Fe, 13.80. Calc. C, 25.8; H, 3.6; S, 45.8; Fe, 13.3.

**In(S<sub>2</sub>COEt)<sub>3</sub>.** Anal. Calc. % (obtained) for  $\text{C}_9\text{H}_{15}\text{S}_6\text{O}_3\text{In}$ : C, 22.60 (22.95); H, 3.16 (2.98); S, 40.13 (39.94); In, 24.00 (23.77).

**Ni(S<sub>2</sub>COEt)<sub>2</sub>.** Elemental analysis for  $\text{C}_6\text{H}_{10}\text{O}_2\text{S}_4\text{Ni}$ : Found: C, 23.81; H, 3.2; S, 42.17; Ni, 20.1%; Calc. C, 23.91; H, 3.35; S, 42.51; Ni, 19.49.

**Sb(S<sub>2</sub>COEt)<sub>3</sub>.** Elemental analysis (%) found for C<sub>9</sub>H<sub>15</sub>S<sub>6</sub>O<sub>3</sub>Sb: C, 22.51; H, 3.07; S, 39.71; Sb, 24.88. Calcd: C, 22.25; H, 3.11; S, 39.55; Sb, 25.1.

**Sn(S<sub>2</sub>COEt)<sub>2</sub>.** Calc. for C<sub>6</sub>H<sub>10</sub>O<sub>2</sub>S<sub>4</sub>Sn (%): C 20.0, H 2.79, S 35.5, Sn 32.9; found: C 19.7, H 2.74, S 35.5, Sn 32.2.



Scheme 1. Pyrolysis of xanthate by Chugaev elimination mechanism.

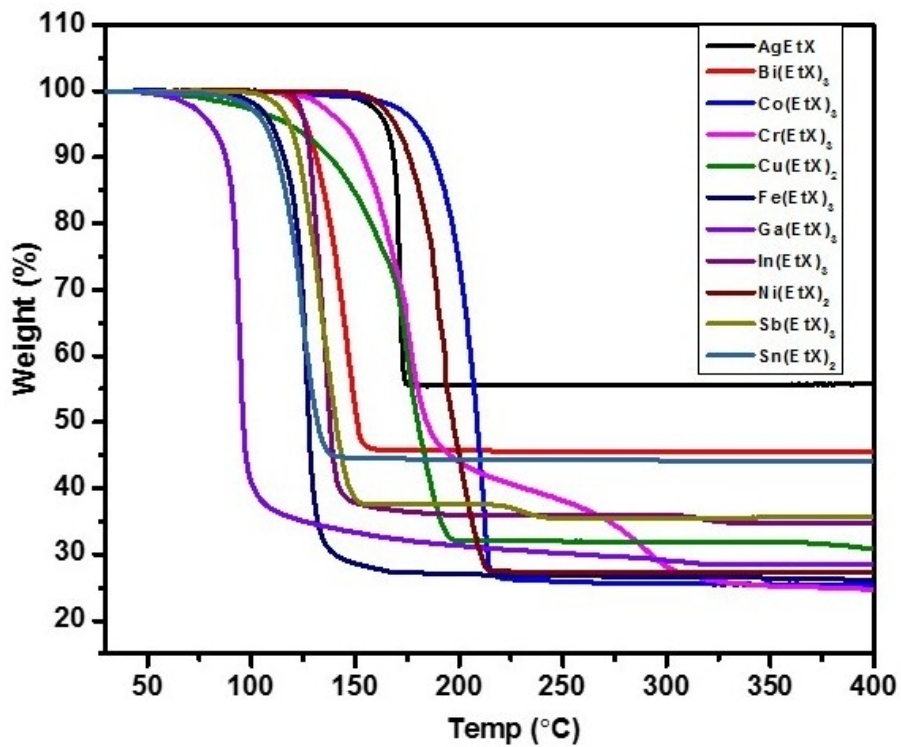


Figure S1 Thermogravimetric analysis of different metal xanthate precursors (where EtX is ethyl xanthate).

Table S1. Onset temperatures of different ethyl xanthate complexes obtained by DSC.

Serial No.	Complex	Onset temperature
1	$\text{Ag}(\text{EtX})$	164 °C
2	$[\text{Bi}(\text{EtX})_3]$	102°C
3	$[\text{Co}(\text{EtX})_3]$	118 °C
4	$[\text{Cr}(\text{EtX})_3]$	124 °C
5	$[\text{Cu}(\text{EtX})_2]$	177 °C
6	$[\text{Fe}(\text{EtX})_3]$	107 °C
7	$[\text{Ga}(\text{EtX})_3]$	95 °C
8	$[\text{In}(\text{EtX})_3]$	126 °C
9	$[\text{Ni}(\text{EtX})_2]$	133 °C
10	$[\text{Sb}(\text{EtX})_3]$	84 °C

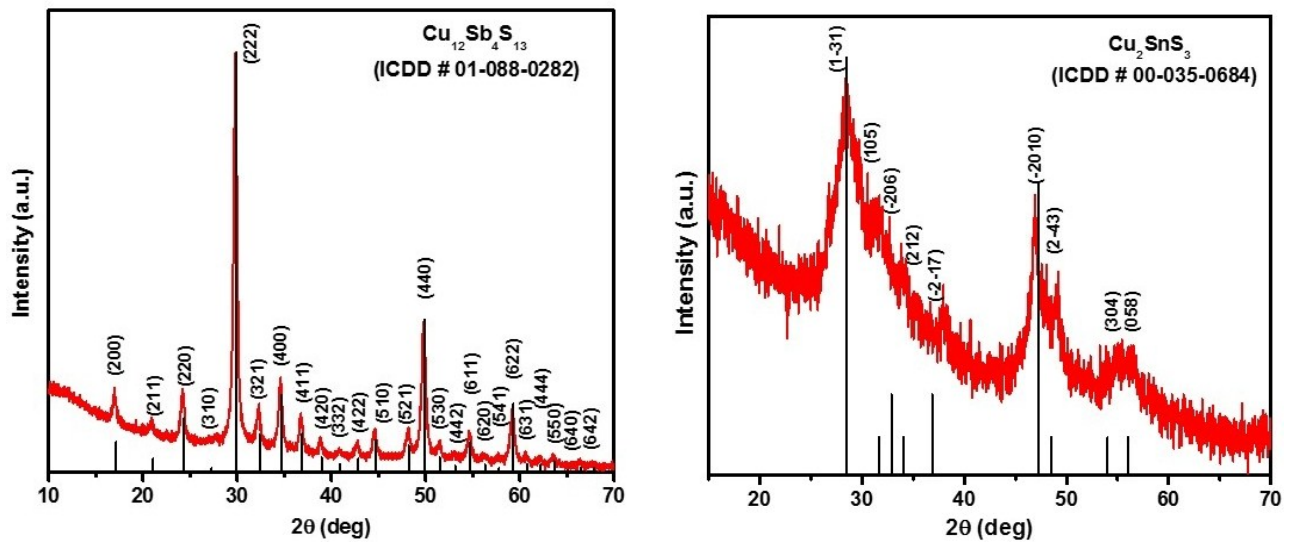


Figure S2 p-XRD pattern of tetrahedrite ( $\text{Cu}_{12}\text{Sb}_4\text{S}_{13}$ ) and mohite ( $\text{Cu}_2\text{SnS}_3$ ) synthesized by melts at 250 °C.

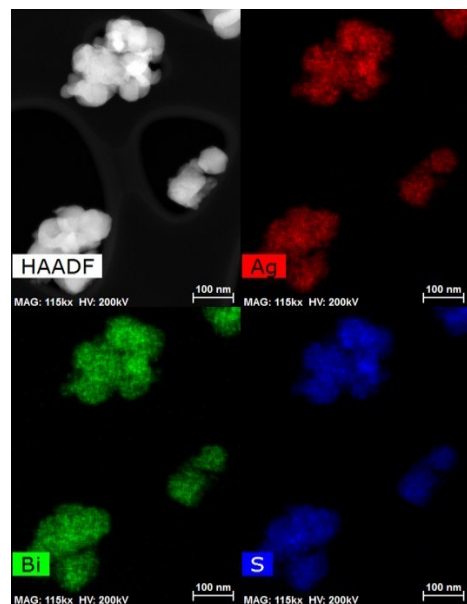


Figure S3 High angle annular dark field (HAADF) image of  $\text{AgBiS}_2$  and elemental mapping of same image, showing a uniform distribution of silver, bismuth and sulfur.

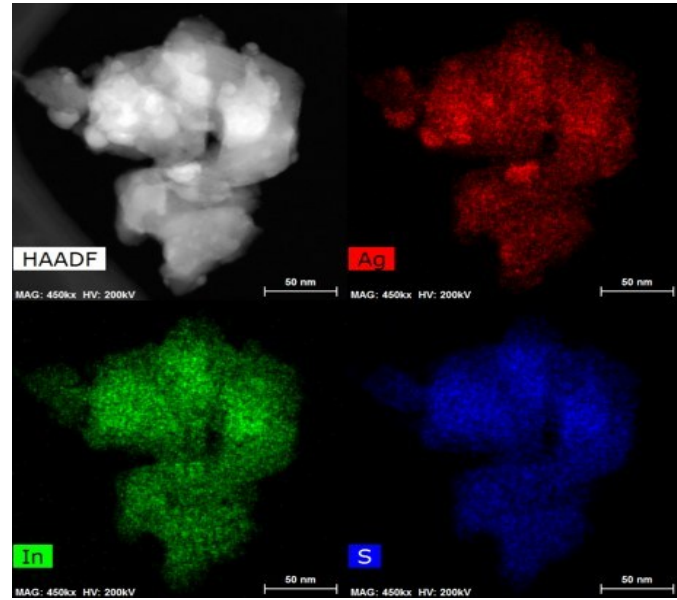


Figure S4      High angle annular dark field (HAADF) image of  $\text{AgInS}_2$  and elemental mapping of same image, showing a uniform distribution of silver, indium and sulfur.

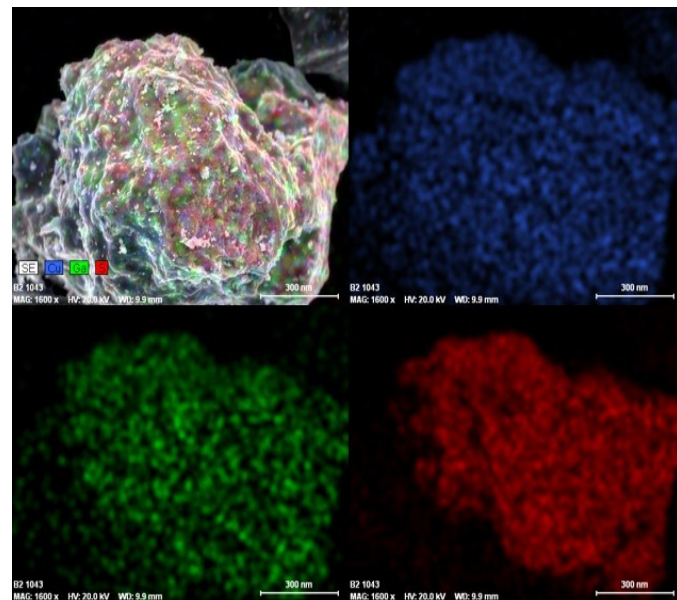


Figure S5      EDX imaging of  $\text{CuGaS}_2$  showing a uniform distribution of copper (blue), gallium (green) and sulfur (red) by SEM.

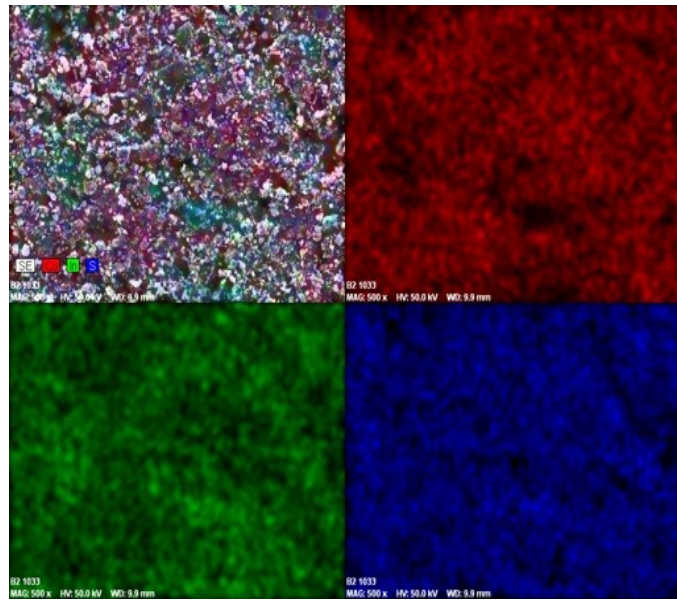


Figure S6 EDX imaging of  $\text{CuInS}_2$  showing a uniform distribution of copper (red), indium (green) and sulfur (blue) by SEM.

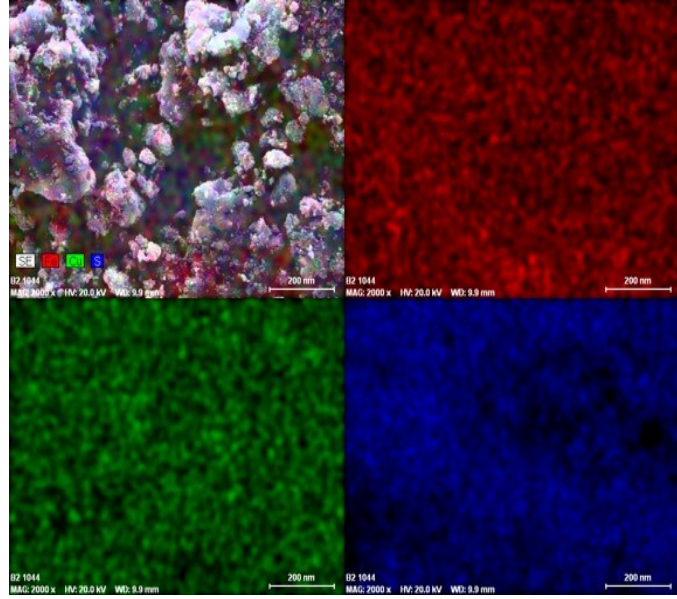


Figure S7 EDX imaging of  $\text{CuFeS}_2$  showing a uniform distribution of copper (green), iron (red) and sulfur (blue) by SEM.

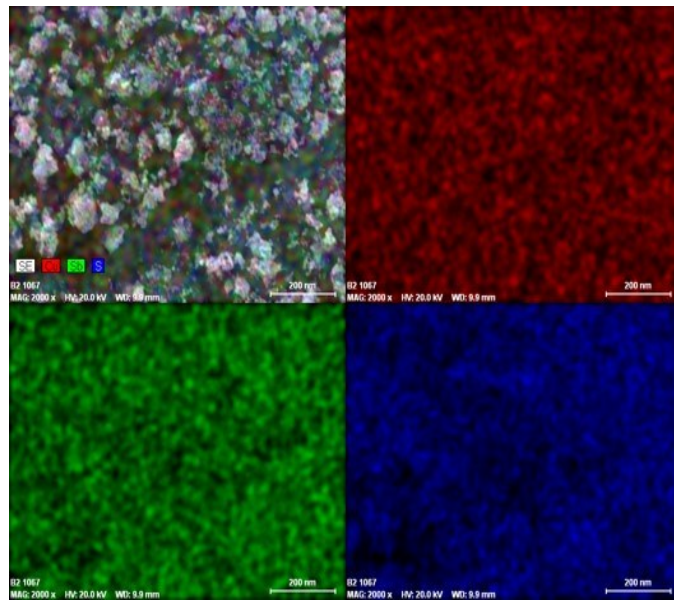


Figure S8 EDX imaging of  $\text{CuSbS}_2$  showing a uniform distribution of copper (red), antimony (green) and sulfur (blue) by SEM.

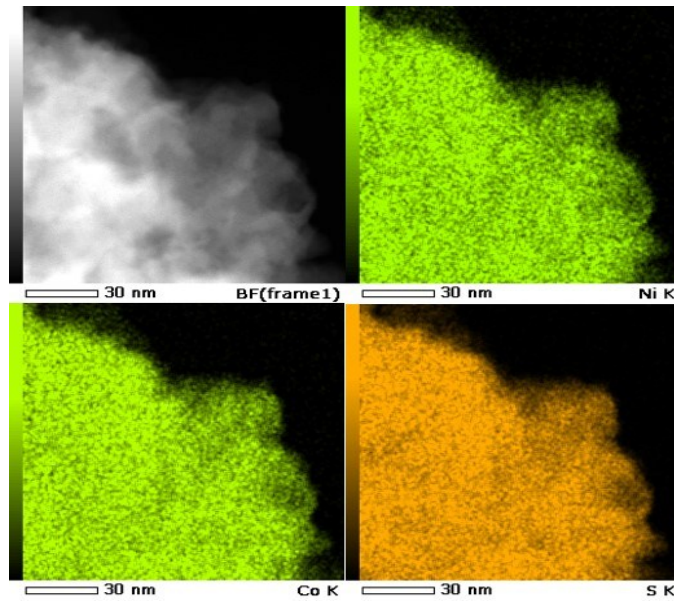


Figure S9 High angle annular dark field (HAADF) image of  $\text{NiCo}_2\text{S}_4$  (thiospinel) and elemental mapping of same image, showing a uniform distribution of nickel, cobalt and sulfur.

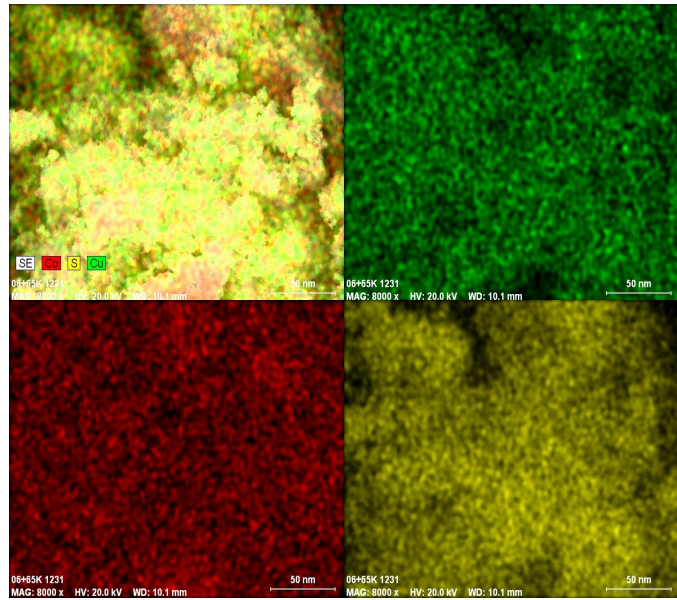


Figure S10 EDX imaging of  $\text{CuCo}_2\text{S}_4$  showing a uniform distribution of copper (green), cobalt (red) and sulfur (yellow) by SEM.

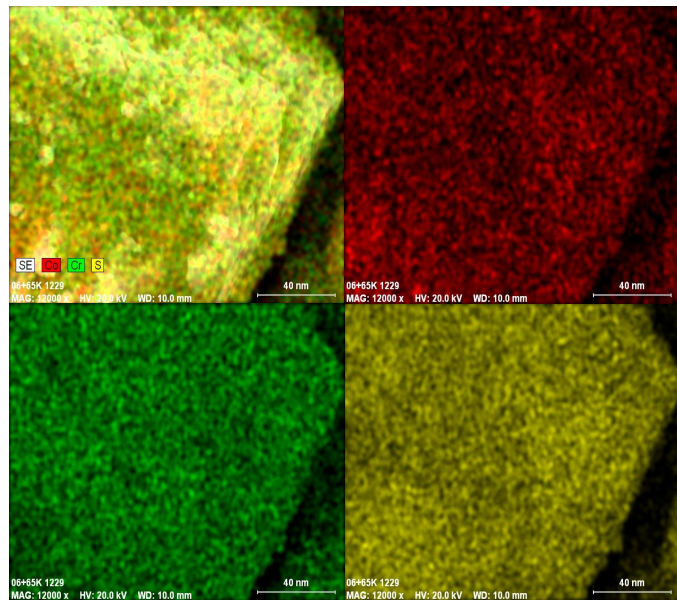


Figure S11 EDX imaging of  $\text{CoCr}_2\text{S}_4$  showing a uniform distribution of cobalt (red), chromium (green) and sulfur (yellow) by SEM.

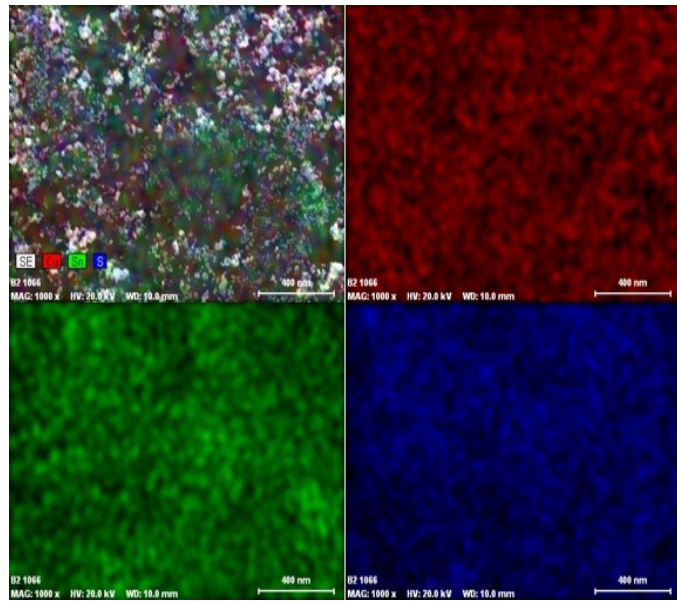


Figure S12 EDX imaging of  $\text{Cu}_2\text{SnS}_3$  showing a uniform distribution of copper (red), tin (green) and sulfur (blue) by SEM.

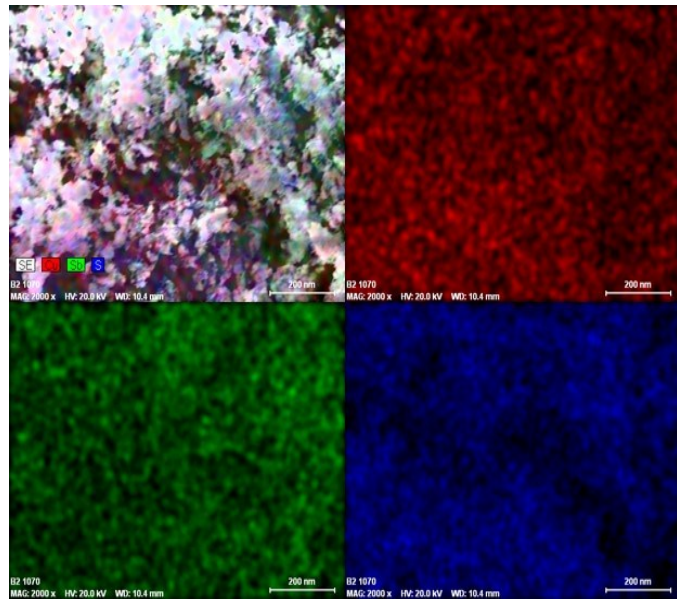


Figure S13 EDX imaging of  $\text{Cu}_{12}\text{Sb}_4\text{S}_{13}$  showing a uniform distribution of copper (red), antimony (green) and sulfur (blue) by SEM.

## References

1. Y. W. Koh, C. S. Lai, A. Y. Du, E. R. Tiekink and K. P. Loh, *Chem. Mater.*, 2003, **15**, 4544-4554.
2. M. Akhtar, M. A. Malik, F. Tuna and P. O'Brien, *J. Mater. Chem. A*, 2013, **1**, 8766-8774.
3. M. Akhtar, Y. Alghamdi, J. Akhtar, Z. Aslam, N. Revaprasadu and M. A. Malik, *Mater. Chem. Phys.*, 2016, **180**, 404-412.
4. S. C. Masikane and N. Revaprasadu, *Mater. Sci. Semicond. Process.*, 2018, **76**, 73-79.
5. D. P. Dutta, G. Sharma and I. Gopalakrishnan, *Mater. Lett.*, 2008, **62**, 1275-1278.
6. C. Zhang, S. Zhang, L. Yu, Z. Zhang, P. Zhang and Z. Wu, *Mater. Lett.*, 2012, **85**, 77-80.
7. M. Al-Shakban, P. D. Matthews, N. Savjani, X. L. Zhong, Y. Wang, M. Missous and P. O'Brien, *J. Mater. Sci.*, 2017, **52**, 12761-12771.
8. G. Watt and B. McCormick, *J. Inorg. Nucl. Chem.*, 1965, **27**, 898-900.
9. M. Akhtar, N. Revaprasadu, M. A. Malik and J. Raftery, *Mater. Sci. Semicond. Process.*, 2015, **30**, 368-375.
10. J. K. Brown, H. D. Arman, P. V. Poplavkin and E. R. Tiekink, *Z. Kristallogr. Cryst. Mater.*, 2009, **224**, 368-374.
11. B. F. Hoskins, E. R. Tiekink, R. Vecchiet and G. Winter, *Inorganica Chim. Acta*, 1984, **90**, 197-200.
12. M. Cox and E. R. T. Tiekink, *Z. Kristallogr.*, 1998, **213**, 487-492.
13. M. Al-Shakban, Z. Xie, N. Savjani, M. A. Malik and P. O'Brien, *J. Mater. Sci.*, 2016, **51**, 6166-6172.